International Journal of Current Engineering and Technology
E-ISSN 2277 – 4106, P-ISSN 2347 – 5161

Available at http://inpressco.com/category/ijcet

Research Article

Static and Dynamic Analysis of the Factors Affecting the Fatigue Life of Heavy Truck Chassis Structure

Seyed Hadi Bayat[#*] and Mohammad Zehsaz[^]

[#]Department of Mechanical Engineering, Isfahan University of Technology, Isfahan, Iran
[^]Department of Mechanical Engineering, Tabriz University, Tabriz, Iran

Received 20 Sept 2017, Accepted 23 Nov 2017, Available online 24 Nov 2017, **Vol.7, No.6 (Nov/Dec 2017)**

Abstract

The study aim is static and dynamic analyze of the parameters affecting the fatigue life of heavy truck chassis structure. A vehicle is made of two parts such as body and chassis. The chassis structure (or chassis frame) has been considered as a base that various components of the vehicle are built based on it and is a combination of longitudinal and transverse elements. In this study, at first a 3D model of heavy truck chassis structure is presented numerically. So, both static and dynamic loads applied on chassis structure consisted of the chassis structures weight and road roughness is calculated and the model is placed under specific boundary conditions and the effect of above loads. The findings of the study indicates that as passing over road roughness with high height or depth, the chassis structure will have a limited life and it has been found that the critical case occurs when only the rear wheels are passing over them.

Keywords: *Heavy truck chassis structure, stress, finite element method, fatigue life, road roughness*

1. Introduction

The chassis as a metal skeleton burned the tasks to run and keep all components of the vehicle and is usually built of hardened steel. Some components of vehicles including body, engine, transmission system, axles, wheels, suspension system, control systems such as braking, steering are installed on this hardened steel and is subjected to static forces due to the weight of these components.

As the vehicles passing through the road, the chassis frame is excited by dynamic forces induced by the road roughness, engine, transmission and more. The truck chassis tends to vibrate in such different dynamic excitations. If any of the excitation frequencies occur simultaneously with the natural frequencies of the vehicle chassis, so resonance events occurs and the chassis will undergo dangerously large oscillations that may lead to additive deflection and failure.

In this regard, static and dynamic analysis of factors affecting the heavy truck chassis is vital to solve these problems. Fatigue damage on chassis is related to various factors such as the quality of roads on which vehicles are driven, vehicle speed and movement type (straight, rolling, breaking, moving along uneven roads) and etc. Then, stress analysis in investigating the fatigue behavior and life expectancy of the chassis is important to determine the location of the highest stress that is known as the critical location and may lead to failure due to fatigue. So, various study carried out by researchers on this field which are described below.

Karaoglu *et al* (2002) addressed the stress analysis of a truck chassis with riveted joints. They examined the effect of connection plate's thickness and side member's thickness to decrease the magnitude of stress around the riveted joints of the chassis frame. Accordingly, the thickness of side member assumed varying from 8 to 12 mm, the thickness of connection plate is altered from 7 to 10 mm and the length of the connection plate is also varied from 390 to 430 mm. By applying finite element method (FEM), the analysis results indicated that increasing the thickness of side member and connection plate can decrease stresses on the joint areas, so the overall weight of the chassis frame increases about 3% and the thickness change of side member is not possible, increasing the connection plate length may be a good alternative to decrease stress but the overall weight of the chassis frame will increase by 4%.

Pinto *et al* (2003) investigated the automotive frame optimization. Their study aimed to obtain an optimized chassis design for an off-road vehicle with the appropriate dynamic and structural behavior performed. In the FEM, chassis has improved by applying steel with closed rectangular profile

*Corresponding author **Seyed Hadi Bayat** (ORCID ID: 0000-0000-0000-0000) is PhD Scholar and **Mohammad Zehsaz** is working as Processor

longitudinal rails and tubular section cross-member. Groups of numerical and programming techniques to search for the optimum value of mathematical functions have been utilized to optimize the frame. The findings of study indicated that the analysis and experimental procedure had significantly improved the overall structural stiffness by 75% by maintaining the center of gravity and the total weight was increased by 6%.

Han Fuiand *et al* (2007) have analyzed the static and dynamic response of a 4.5 ton truck chassis due to road roughness. Vibration induced by road roughness and excitation by the vibrating components imposed on chassis were examined. Chassis responses were examined by stress distribution and displacements. Mode shape results determine the suitable mounting locations of components such as engine and suspension systems. Analysis results show that the road excitation was main disturbance to the chassis.

Zehsaz *et al* (2008) investigated the effect of connection plate thickness on stress of a semi-heavy truck chassis with riveted and welded joints under dynamic loads due to road roughness by using Finite Element Method (FEM) and the modes of chassis vibration, natural frequencies and modal shapes have been calculated based on the FE analysis to validate the FE model of the chassis, and were compared with the results of experimental modal analysis. The strength of the welded and combined welded-riveted joints has been addressed with three different plate thicknesses to ensure the effect of the connection plate's thickness on the strength of the chassis. The findings of study show that the amount of stresses in chassis and connection plates are decreased significantly with increasing the thickness of connection plates and also combined welded-riveted joints reduces the stress level of the chassis.

Hosseini *et al* (2011) carried a dynamic analysis on a modified truck chassis. The 6 ton truck model has been simulated with appropriate accuracy and based on the effect of bolted and riveted joints. Modal analysis (finding the natural frequencies and mode shapes by using free-free boundary condition) using numerical finite element method has been accomplished. Their analysis showed that in the first, second and sixth modes with natural frequencies less than 40 Hz, the vibrations of the truck chassis consisted of torsion and vertical bending that the local bending vibration occurs at the top hat cross member where the gearbox is mounted on it. So, chassis mass increases according to the installed equipment, the natural frequencies fall out of the natural range that can be compensated with increasing the chassis stiffness and decreasing the chassis length, can increase the chassis stiffness.

Kashyzadeh *et al* (2013) studied the effect of vehicle speed on simulated road roughness. So, at high speeds it is possible to jump over some of the bump points on the road, hence the speed of the vehicle will be influenced the same road roughness to the vehicle. So, 3 levels of vehicle speeds 34, 70 and 100 km/h have been utilized. Also, study of the effect of road roughness on vehicle components has been examined. The results of study show that high and low speeds have the same effect on road roughness in excellent road conditions and in poor road conditions, the impact of high speed is more than the low speed

Zehsaz *et al* (2015) examined the fatigue life of a semi-heavy truck chassis under dynamic loads such as road roughness, braking and cornering. The study aim is to provide a solution based on FEM to determining the fatigue life in chassis design of a semi-heavy truck, calculating the natural frequencies and mode shapes and comparing them with the experimental modal analysis and providing a method for simulating road roughness in the time domain according to the international reference index (IRI). By considering different road types with potholes and kerbs and different load conditions (braking and cornering), they confirmed that numerical method has sufficient accuracy and reliability. It also concluded that the semi-heavy truck chassis is under bending and torsional loads as moving through the bumps and the critical case occurs when one pair of a front wheel and a rear wheel on the opposite side are driving over kerbs.

Rao *et al* (2016) have been examined a crack growth in a heavy duty truck frame rail and its failure process. In this study, dynamic loads used a full vehicle model to modeled the crack growth in the chassis frame and it show that an aggressively drilled open hole built small crack initiations in a high stress-state location of the frame, which resulted in extensive curvilinear crack growth under dynamic loads of the vehicle and its location was on the frame web within the torque rod connection to the rear drive axle of the vehicle.

2. Chassis and suspension model

The heavy vehicle chassis of the Mercedes-Benz Actros is built of ASTM A710 steel that its specifications are shown in the tables 1 and 2.

Table 1 Physical specifications of heavy vehicle chassis

Material	Modulus of elasticity (GPa)	Density (kg/m3)	Tensile strength (MPa)	Yield strength (MPa)
ASTM A710 Steel	205	7850	515	450

Table 2 Specification of heavy vehicle chassis frame

S. No.	Parameters	Value
1	Total length of the chassis	9190 mm
2	Width of the chassis	920 mm
3	Wheel Base	4500 mm
4	Front Overhang	1440 mm
5	Rear Overhang	1900 mm
6	Ground Clearance	344 mm
7	Capacity (GVW)	33 ton

In this study, CAE software CATIA V5 used to create a 3D solid model of the heavy vehicle chassis. At first the parts of model used to create the model accurately, and then they are assembled to make complete geometric model. The finite element solver ANSYS 17.2 used to analyses the model created in CATIA V5. ANSYS is a general purpose finite element analysis (FEA) software package. So the geometric model created in CATIA is implemented in ANSYS. It is notable that in heavy vehicle chassis modeling, cross members are connected by welded joints to the side members of the chassis and the dimensions of the members used in the modeling and assembly are shown below.

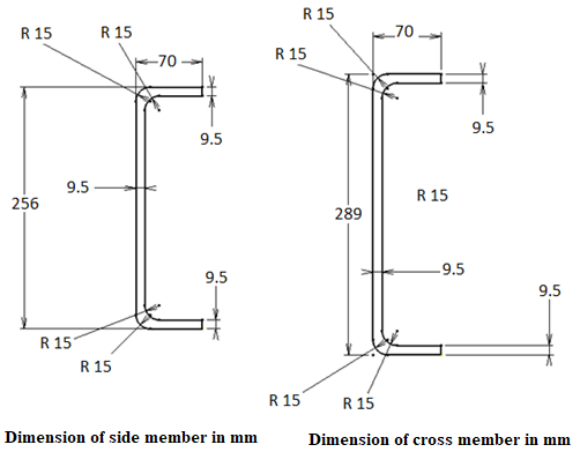

Fig. 1. Dimension of side and cross members of channel section

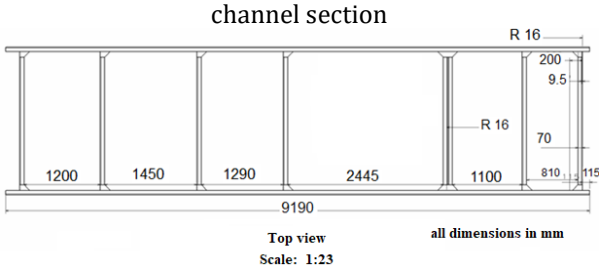

Fig. 2. Front and side view

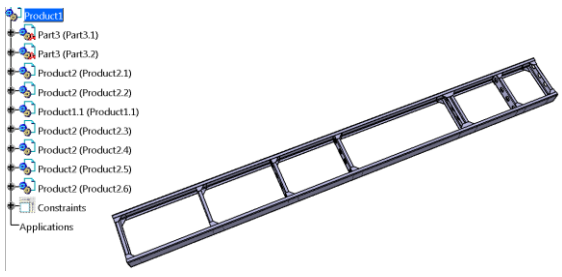

Fig. 3. Assembled chassis frame in CATIA

The excessive oscillations of chassis and suspension occur as the vehicle moving through uneven road surfaces. This oscillation that initially used to the wheels and suspension system is a function of several factors such as: vehicle mass, speed, suspension type, road surface irregularities, etc. So, the QCM (Quarter Car Model, see Fig. 4) is the vehicle model that can effectively be used to study the dynamic interaction between vehicle and road roughness profile. The quarter-car model differential equations under Newton's law of motion by combining the masses values m, the stiffness constant k and damping c written to determine the vertical displacement of sprung mass (z) against excitations caused by the road roughness (h) as follows:

$$m_s\ddot{z} = -C_s(\dot{z} - \dot{y}) - k_s(z - y) \quad (1)$$

$$m_u\ddot{y} = -C_s(\dot{y} - \dot{z}) - k_s(y - z) - k_t(y - h) \quad (2)$$

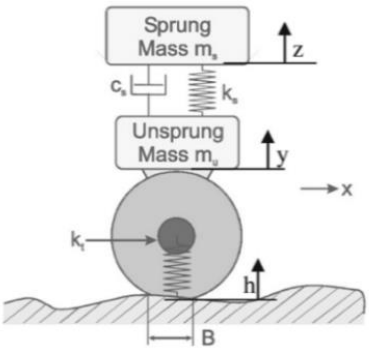

Fig. 4. Quarter car model

The parameters of the heavy truck: tire mass m_u is 100kg, mass on spring m_s is 9200kg, suspension stiffness k_s is 5000000$\frac{N}{m}$, tire stiffness $k_t$is 500000 $\frac{N}{m}$, suspension damping C is 1500 $\frac{Ns}{m}$. Then the two above equations are simulated in the Simulink of MATLAB software using different blocks. The Simulink environment is used to modeling, simulating and analyzing dynamic systems and supports linear and nonlinear systems. In this environment, the user will be able to simulate and execute a system by blocks and use the results for different purposes. The output of the above system is the vertical acceleration of sprung mass, which can be used to obtain the dynamic force.

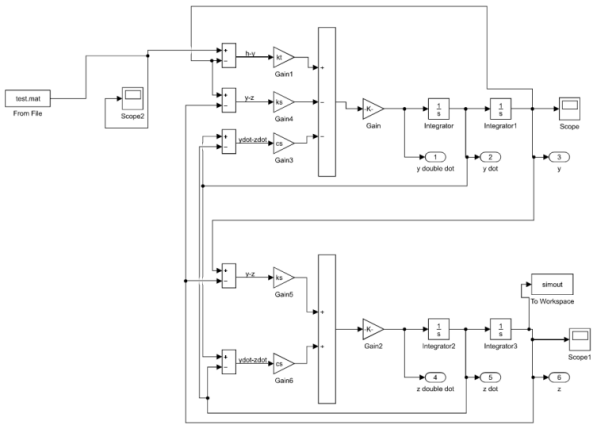

Fig. 5. Simulation of a quarter car model in the Simulink environment of MATLAB software

3. Simulation of road roughnesses

3.1 Simulation of different road classes

When the vehicle moves through the road, irritation caused by uneven road used to the suspension and so the chassis through the front and rear wheels. For practical applications, in agreement with the ISO road roughness surfaces classification, it is possible to create an artificial road profile from a stochastic representation, in terms of the function of Power Spectral Density (PSD) of vertical displacements obtained through the Fourier Transform.

Table 3 ISO 8608 values of $G_d(n_o)$ and $G_d(\Omega_o)$

Road class	$G_d(n_0)$ (10^{-6} m^3)		$G_d(\Omega_0)$ (10^{-6} m^3)	
	Lower limit	Upper limit	Lower limit	Upper limit
A	–	32	–	2
B	32	128	2	8
C	128	512	8	32
D	512	2048	32	128
E	2048	8192	128	512
F	8192	32768	512	2048
G	32768	131072	2048	8192
H	131072	–	8192	–
	n_0=0.1 cycles/m		Ω_0=1 rad/m	

In simulations, according to the ISO 8608 the roughness profile of the road surface can be defined as follow:

$$G_d(n) = G_d(n_o) \times (\frac{n}{n_o})^{-2} \quad (3)$$

$$G_d(\Omega) = G_d(\Omega_o) \times (\frac{\Omega}{\Omega_o})^{-2} \quad (4)$$

Where the values of $G_d(n_o)$ and $G_d(\Omega_o)$ must be derived from Table 3 in term of the given road class.
For a given value of spatial frequency n, cantered within a frequency band Δn, the value of the Power Spectral Density function for the assigned frequency n is determined through the following expression:

$$G_d(n) = \lim_{\Delta n \to 0} \frac{\Psi_x^2}{\Delta n} \quad (5)$$

where Ψ_x^2 is the mean square value of the component of the signal for the spatial frequency n, within the frequency band Δn. The road profile signal is conveniently discretized and therefore it is described as a sequence of elevation points uniformly spaced. If the length of road profile is L and the sampling interval is B, the maximum theoretical sampling spatial frequency is $n_{max} = \frac{1}{B}$ and the maximum effective sampling spatial frequency is $n_{eff} = \frac{n_{max}}{2}$and, within the frequency domain, discretized spatial frequency values $n_i$are equally spaced with an interval of $\Delta n = \frac{1}{L}$.

The generic spatial frequency value n_i can be written in the discrete form:

$$G_d(n_i) = \frac{\Psi_x^2(n_i,\Delta n)}{\Delta n} = \frac{\Psi_x^2(i.\Delta n,\Delta n)}{\Delta n} \quad (6)$$

with i varying from 0 to N = $\frac{n_{max}}{\Delta n}$.

If the road profile can be described through a simple harmonic function according to:

$$h(x) = A_i co\,s(2\pi.n_i.x + \varphi) = A_i co\,s(2\pi.i.\Delta n.x + \varphi) \quad (7)$$

Where A_i is the amplitude, n_i is the spatial frequency and φ is the phase angle, it is possible to show that the mean square value of this harmonic signal is as follow:

$$\Psi_x^2 = \frac{{A_i}^2}{2} \quad (8)$$

So we have:

$$G_d(n_i) = \frac{\Psi_x^2(n_i)}{\Delta n} = \frac{{A_i}^2}{2\times\Delta n} \quad (9)$$

If the PSD function of vertical displacements is known, it is possible to create an artificial road profile using the above expression and assuming a random phase angle φ_i following an uniform probabilistic distribution within the 0-2π range. The artificial profile can be described as:

$$h(x) = \sum_{i=0}^{N} A_i co\,s(2\pi.n_i.x + \varphi_i) = \sum_{i=0}^{N} \sqrt{2\times\Delta n.G_d(i.\Delta n)} \times cos(2\pi.i.\Delta n.x + \varphi_i) \quad (10)$$

So, an artificial road profile from ISO classification can be generated by the following equation:

$$h(x) = \sum_{i=0}^{N} \sqrt{\Delta n}.2^k.10^{-3}.\left(\frac{n_o}{i.\Delta n}\right).cos(2\pi.i.\Delta n.x + \varphi_i) \quad (11)$$

Where x is the abscissa variable from 0 to L; $\Delta n = \frac{1}{L}$; $n_{max} = \frac{1}{B}$; N = $\frac{n_{max}}{\Delta n} = \frac{L}{B}$; k is a constant value depending from ISO road profile classification, it assumes integers increasing from 3 to 9, corresponding to the profiles from class A to class H (see Table 4); $n_o = \frac{1}{10}\frac{cycles}{m}$; φ_i random phase angle following uniform probabilistic distribution within the 0–2π range.

So the artificial road profile equation in MATLAB software used for a road section pavement of length equal to 250 m, sampling interval 2500 and for different k values in accordance with the ISO 8608,road roughness created for various road classes (rough, average and very poor roads) at different traveling speeds.

Table 4 k values for ISO road roughness classification

Road Class		k
Upper limit	Lower limit	
A	B	3
B	C	4
C	D	5
D	E	6
E	F	7
F	G	8
G	H	9

Finally, dynamic analysis has been used to simulate this mode in ANSYS software so that using a quarter car models and applying the above excitations as system input that output is the dynamic force applied to the chassis in terms of time, also it is applied to the junction area of wheels' axis. The truck should be constrained in three directions to prevent the rigid motion of the model. Also, because the truck does not rotate around the perpendicular axis of its body (yaw), the truck rotation, the motion of the longitudinal and lateral directions should be restricted.

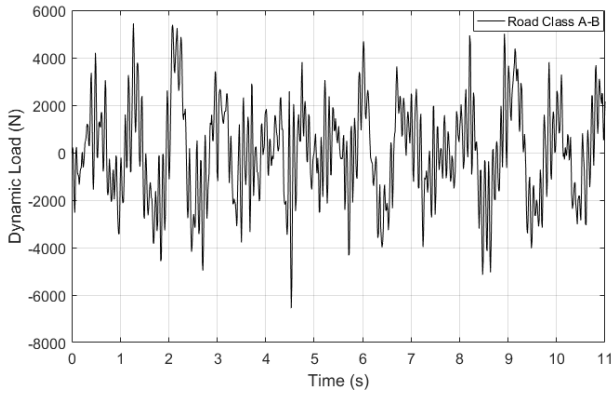

Fig. 6 Dynamic force applied to the chassis in terms of time on rough road at speed 80 km/h

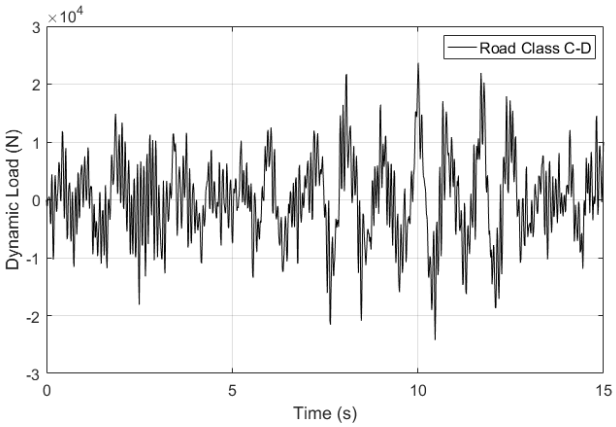

Fig. 7 Dynamic force applied to the chassis in terms of time on average road at speed 60 km/h

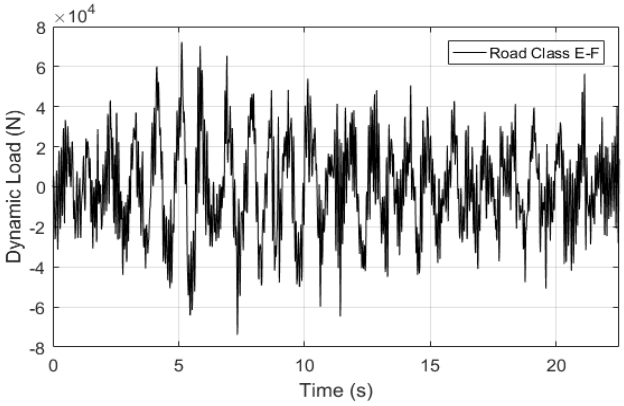

Fig. 8 Dynamic force applied to the chassis in terms of time on very poor road at speed 40 km/h

3.2 Simulation of bump

Bumps are used to force the driver to slow down the vehicle in residential areas (speed hump) and usually have a height of between 50 and 150 mm and a length of 0.3 to 3 meter. Most cars can safely pass through them at speeds of 25 to 30 km/h. The usual bump is shown below:

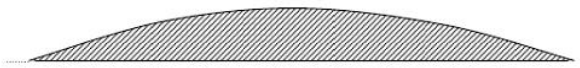

Fig. 9. The usual bump profile on the roads

In this case, the bump profile is determined by the following equation:

$$y = h \times \sin(\omega t) \qquad 0 \le t \le T \tag{12}$$

Where h is the bump height, ω is the angular displacement frequency and T is the time taken by the vehicle to pass the bump.

The angular frequency ω is defined by wave length τ as:

$$\omega = \frac{2\pi}{\tau} = \frac{\pi}{T} \tag{13}$$

Time T is related to the speed of the vehicle (in terms of km/h) as follows:

$$T = \frac{L}{\frac{1000 \times V}{3600}} = \frac{3/6\, L}{V} \tag{14}$$

By combining the two equations we will have:

$$\omega = \frac{\pi V}{3/6\, L} \quad \left(\frac{rad}{s}\right) \tag{15}$$

Thus, the bump profile of the road simulated for the length of 3 m and height of 50, 100 and 200 mm using Matlab software for the vehicle speed of 25 km/hand then using the quarter car model and applying the

above excitations as input of the system in terms of traveling time with speed at 25 km/h, the dynamic force applied to the chassis is obtained in terms of time which is shown in the figures below. Boundary conditions are similar to the previous case.

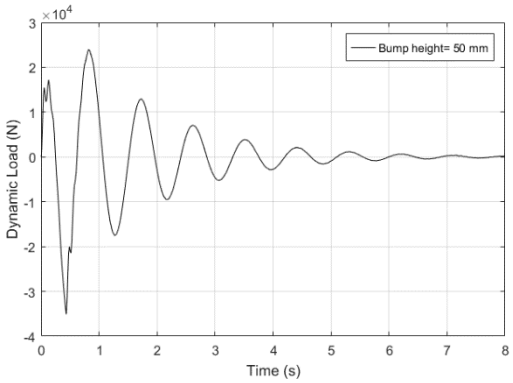

Fig. 10 Dynamic force applied to the chassis in terms of time at bump height of 50 mm

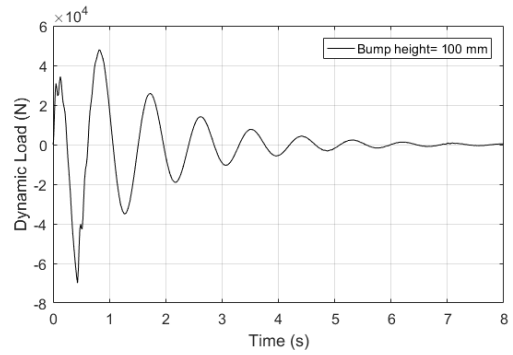

Fig. 11 Dynamic force applied to the chassis in terms of time at bump height of 100 mm

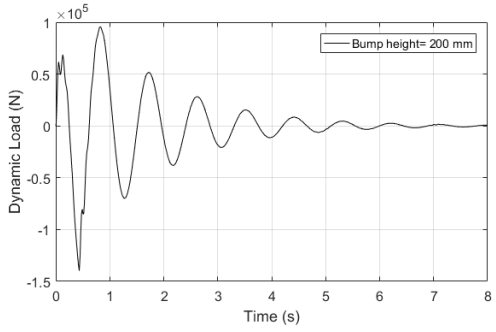

Fig. 12 Dynamic force applied to the chassis in terms of time at bump height of 200 mm

3.3 Simulation of potholes

Potholes are a type of failure in asphalt pavement caused by the presence of water in the underlying soil structure and presence of traffic passing over the affected area. Potholes can grow to several feet in width, though they usually only develop to depths of a few inches. If they become large enough, they can cause damage to tires, wheels and vehicle suspensions and also road accidents.

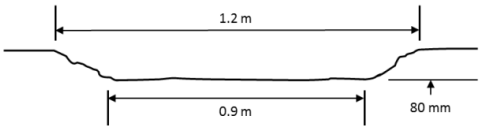

Fig. 13 Pothole profile

Figure 13 shows a typical pothole profile. Potholes can be of various shapes, sizes and geometrical properties. There are no standards for pothole classification in term of size and dimensions other than a description of severity based on depth. For this reason, pothole profile dimensions obtained through experimentation were used for simulations that an example of this is given in table 5.

Table 5 Road surface assessment of pothole severity by close range digital photogrammetry method

Specimen Name	Diameter (m)	Area (m^2)	Depth (mm)
P1	0.575	0.26	79
P2	0.4	0.13	60
P3	1.25	1.23	96
P4	0.915	0.37	59
P5	0.886	0.28	75
P6	1.24	1.21	96
P7	0.915	0.37	59
P8	0.866	0.28	75
P9	0.757	0.45	89
P10	0.556	0.24	90

Then using the quarter car model and using the above excitations as input of the system in terms of traveling time according to the speed of vehicle passing on them, which is 25 km/h, the dynamic force applied to the chassis is obtained in terms of time which is shown in the figures 14, 15 and 16. Boundary conditions are similar to the previous cases.

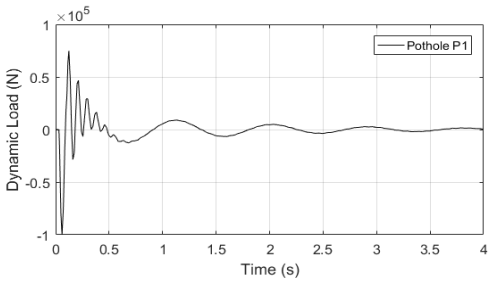

Fig. 14 Dynamic force for the chassis in terms of time in pothole P1

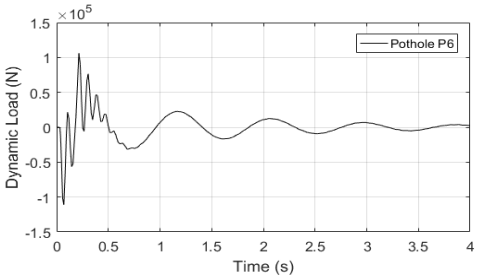

Fig. 15 Dynamic force for the chassis in terms of time in pothole P6

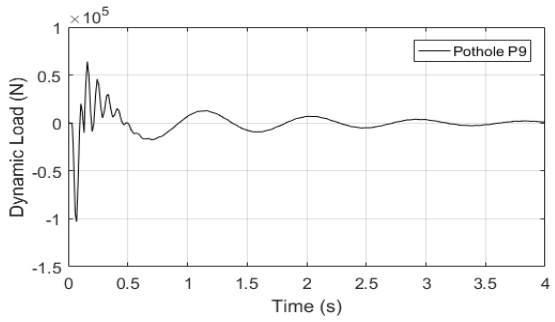

Fig. 16 Dynamic force for the chassis in terms of time in pothole P9

4. Discussion and conclusion

4.1 Simulation of the weight force

According to the capacity of truck to the chassis frame, the result of study shows that the maximum stress on the entire chassis is 138.43 MPa, which is at the rear of the chassis and near the rear wheel axle and the largest displacement is 28.9 mm, which is at the rear of the chassis.

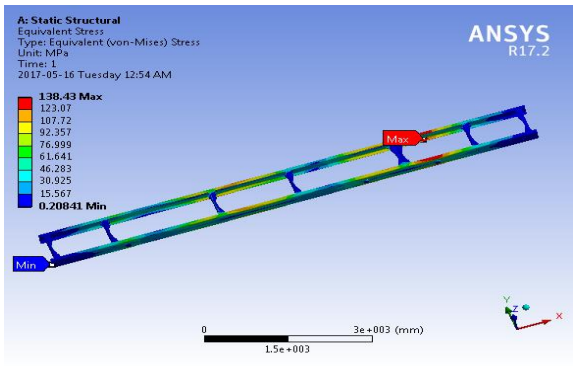

Fig. 17. Stress distributions in term of maximum weight load

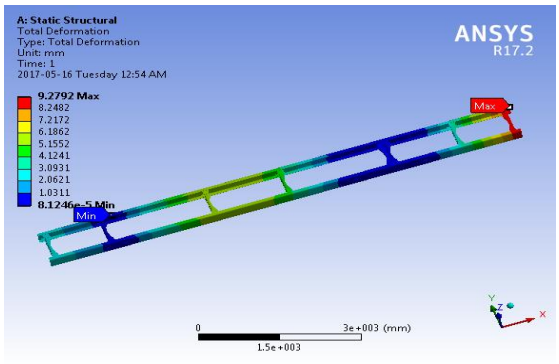

Fig. 18. Displacement pattern in term of maximum weight load

4.2 Fatigue life as moving through the bump

The fatigue endurance limit is determined by considering the correction coefficients to calculate the life of the chassis structure, as follows:

$$S_e = 0.86 \times 0.95 \times S'_e = 0.86 \times 0.95 \times 0.5 \times 515 \approx 231.75\ MPa$$

If the maximum stress is at the area of welding joints, the fatigue endurance limits determined by considering the weld correction coefficient as follows:

$$S_e = 0.65 \times 0.95 \times S'_e = 0.65 \times 0.95 \times 0.5 \times 515 \approx 197.375\ MPa$$

In the case of variable amplitude loading, the stress amplitude of σ_{a1} is applied for the cycles N_1 and so Miner's law show that fatigue failure occurs when the following fractions are equal to one:

$$\frac{N_1}{N_{f1}} + \frac{N_2}{N_{f2}} + \frac{N_3}{N_{f3}} + \cdots = \sum \frac{N_j}{N_{fj}} = 1 \qquad (16)$$

The simulation of moving through bumps at three different heights of 50, 100 and 200 mm was carried out using the dynamic force obtained by simulating the quarter-car model in three cases as follows:

1- First case: Only the front wheels pass over the bump.
2. Second case: Only the rear wheels pass over the bump (with time delay $t_{delay} = \frac{L}{V}$)
3- Third case: All the wheels simultaneously pass over the bump (with time delay $t_{delay} = \frac{L}{V}$)
The location of this critical stress in these three different cases is shown in the following figures.

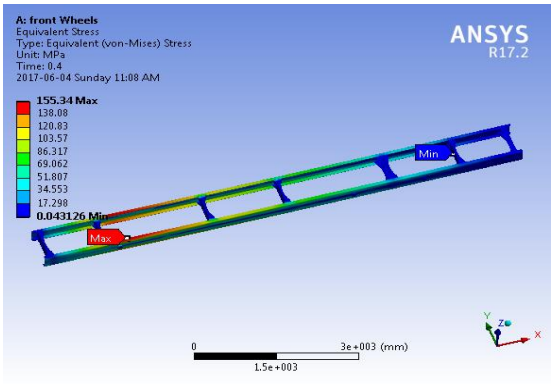

Fig. 19 The location of critical stress in all three different bumps height in the first case

Fig. 20 The location of critical stress in all three different bumps height in the second case

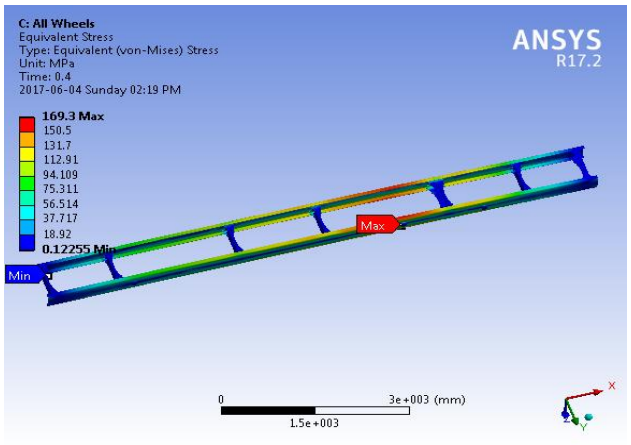

Fig. 21. The location of critical stress in all three different bumps height in the third case

The fatigue life based on Miner's rule in these three cases is presented in the table below.

Table 6 Comparison of chassis fatigue life in simulating road bump in three different cases

	Bump height (mm)	Maximum stress in chassis frame	Fatigue life (number of blocks)
First Case	50	155.34	Unlimited Life
	100	194.2	
	200	277.77	25223
Second Case	50	194.25	Unlimited Life
	100	234.6	59950
	200	435	1049
Third Case	50	169.3	Unlimited Life
	100	213.86	
	200	306.55	15068

4.3 Fatigue life when moving through the pothole

Moving through the pothole in three different pothole samples modeled using the dynamic force obtained by simulating a quarter-car model in three cases as follows:

1- First case: Only the front wheels pass over the pothole.

2. Second case: Only the rear wheels pass over the pothole (with time delay $t_{delay} = \frac{L}{V}$)

3- Third case: All the wheels simultaneously pass over the pothole (with time delay $t_{delay} = \frac{L}{V}$)

The location of this critical stress in these three different cases is shown in the following figures.

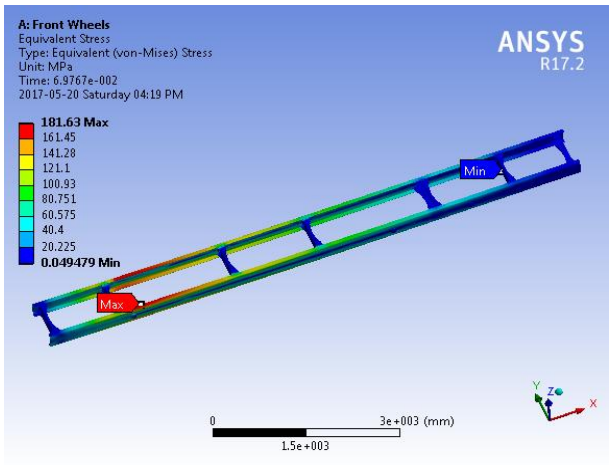

Fig. 22 The location of critical stress in all three samples of pothole in the first case

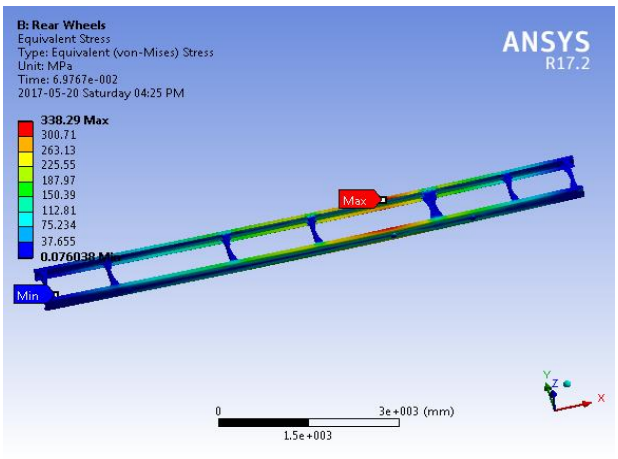

Fig. 23 The location of critical stress in all three samples of pothole in the second case

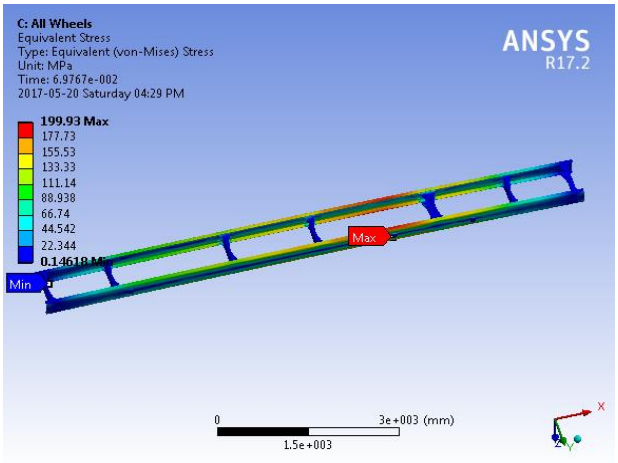

Fig. 24 The location of critical stress in all three samples of pothole in the third case

The fatigue life based on Miner's rule in these three cases is presented in the table 7. These results show that the most critical condition is for the pothole sample P6.

Table 7 Comparison of chassis fatigue life in simulating road potholes in three different cases

	Pothole Sample	Maximum stress in chassis frame	Fatigue life (number of blocks)
First Case	P1	181.63	Unlimited Life
	P6	251.7	42090
	P9	233.28	61652
Second Case	P1	338.29	9007
	P6	442	1471
	P9	416.67	2256
Third Case	P1	199.93	Unlimited Life
	P6	277.6	25304
	P9	257.17	37711

4.4 Fatigue life in simulating three different road classes

Dynamic force obtained by the quarter car model used to simulate uneven roads in three different classes. In this case, the force is first applied to the front axle and then with the time $t_{delay} = \frac{L}{V}$, where L is the distance between the two rear axles and V is the speed of the vehicle, it is also applied to the rear axles.

In this case, the maximum stress generated on the chassis in ISO road A-B, C-D and E-F were 156.4, 172.26, and 366.22 MPa, respectively which is shown in the figures below. The location of the critical stress in these three different road classes is at the rear of the chassis (near the rear wheels' axle), which is shown in the fig. 26. The most critical condition is for the road class E-F (very poor road).

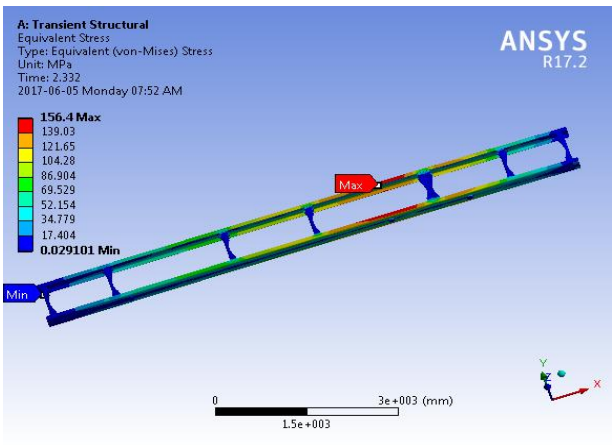

Fig. 26. The location of the critical stress in three different road classes

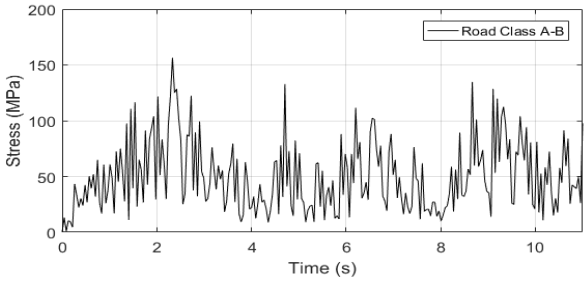

Fig. 27. Stress level (Von-Mises) on rough road at speed 80 km/h

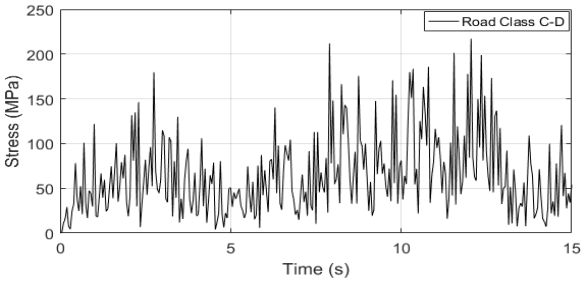

Fig. 28. Stress level (Von-Mises) on average road at speed 60 km/h

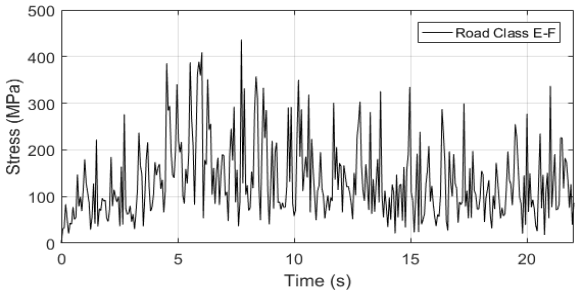

Fig. 28. Stress level (Von-Mises) on very poor road at speed 40 km/h

The fatigue life based on Miner's rule in these three different road classes is given in the table below.

Table 4 The maximum stress on the chassis in term of road roughness in three different road classes

Road type	Maximum stress in chassis frame	Fatigue life (number of blocks)
Rough road (Class A-B)	156.4	Unlimited Life
Average road (Class C-D)	217.16	87512
Very poor road (Class E-F)	436.22	2271

Conclusion

The study aim is to analysis a heavy vehicle chassis structure using numerical method of FEM. In this

regard, different parts of the chassis and weld connections are modeled in CATIA and then entered into ANSYS software and were meshed. Afterwards, static and dynamic forces such as weight force and forces caused by road roughness were examined and applied to the model. Road roughness was also simulated based on the ISO 8608 and the dynamic forces applied to the chassis frame were extracted using simulation of a quarter-car model during a motion of constant speed. The results show that at bump height of 20 cm and more, the critical stresses are greater than the fatigue endurance limit and the chassis will have a limited life and the critical case occurs when only the rear wheels are moving through the bump. Also passing over all three pothole samples caused a lot of stress to the chassis that reduce its life and the critical case occurs when the pothole depth is 90 mm and more. In simulating very poor road profile (class E-F) and apply it to the quarter car model and extraction of dynamically applied forces on the chassis structure, the results of study show that in this case the chassis was found to be under too much stress (which is directly related to the increase in vehicle speed) and caused its life to be reduced.

References

T. H. Fui and R. A Rahman (2007), Statics and dynamics structural analysis of a 4.5 ton truck chassis, *Jurnal Mekanikal,* vol. 24, pp. 56-67.

C. Karaoğlu and N. S. Kuralay (2002), Stress analysis of a truck chassis with riveted joints, *Finite Elements in Analysis and Design,* vol. 38, no. 12, pp. 1115-1130.

F. Pinto, J. C. Rezende, L. M. Freitas, and J. A. Borges (2003), Automotive Frame Optimization, presented at the 12th International Mobility Technology Congress and Exhibition, Sao Paulo, Brazil.

M. Zehsaz, F. V. Tahami, and F. Esmaeili (2009), The Effect of Connection-Plate Thickness on Stress of Truck Chassis with Riveted and Welded Joints under Dynamic Loads, *Asian Journal of Applied Sciences,* vol. 2, no. 1, pp. 22-35.

M. Forouzan and R. Hoseini (2011), Dynamic Analysis of a Modified Truck Chassis, *International Journal of Advanced Design and Manufacturing Technology,* vol. 3, no. 4, pp. 31-36.

K. Reza-Kashyzadeh, M. J. Ostad-Ahmad-Ghorabi, and A. Arghavan (2013), Study Effects of Vehicle Velocity on A Road Surface Roughness Simulation, in *Applied Mechanics and Materials*, vol. 372, pp. 650-656: Trans Tech Publ.

M. Zehsaz, M. H. Sadeghi, M. M. Ettefagh, and R. Hassannejad (2015), Fatigue Strength of a Chassis of a Semi-Heavy Truck under Dynamic Loads due to Real Road Roughness, *Transactions of FAMENA,* vol. 38, no. 4, pp. 89-105.

V. N. Rao and J. W. Eischen (2016), Failure analysis of mixed mode crack growth in heavy duty truck frame rail, *Case Studies in Engineering Failure Analysis,* vol. 5, pp. 67-74.

N. Nickmehr (2011), Ride quality and drivability of a typical passenger car subject to engine/driveline and road non-uniformities excitations, ed.

M. Agostinacchio, D. Ciampa, and S. Olita (2014), The vibrations induced by surface irregularities in road pavements–a Matlab® approach, *European Transport Research Review,* vol. 6, no. 3, pp. 267-275.

H. G.A. (2015), Car Dynamics using Quarter Model and Passive Suspension, *Journal of Mechanical and Civil Engineering,* vol. 12, no. 1, pp. 51-5.

A. M. Rao (2016), A Structured Approach to Defining Active Suspension Requirements, Virginia Tech.

P. L. Y. Tiong, M. Mustaffar, and M. R. Hainin (2012), Road surface assessment of pothole severity by close range digital photogrammetry method, *World Appl Sci J,* vol. 19, no. 6, pp. 867-873